JOURNAL OF Applied Polymer SCIENCE

Thermosensitive Self-Assembly Micelles from A_2BA_2-Type Poly(*N*-isopropyl acrylamide)$_2$-*b*-Poly(lactic acid)-*b*-Poly(*N*-isopropyl acrylamide)$_2$ Four-Armed Star Block Copolymers and Their Applications as Drug Carriers

Yan-Ling Luo, Xiao-Li Yang, Feng Xu, Ya-Shao Chen, Zhuo-Ma Ren-Ting

Key Laboratory of Macromolecular Science of Shaanxi Province, School of Chemistry and Chemical Engineering, Shaanxi Normal University, Xi'an 710062, People's Republic of China

Correspondence to: Y.-L. Luo (E-mail: luoyanl@snnu.edu.cn) or F. Xu (E-mail: fengxu@snnu.edu.cn)

ABSTRACT: A novel A_2BA_2-type thermosensitive four-armed star block copolymer, poly(*N*-isopropyl acrylamide)$_2$-*b*-poly(lactic acid)-*b*-poly(*N*-isopropyl acrylamide)$_2$, was synthesized by atom transfer radical polymerization and characterized by ^{1}H-NMR, Fourier transform infrared spectroscopy, and size exclusion chromatography. The copolymers can self-assemble into nanoscale spherical core–shell micelles. Dynamic light scattering, surface tension, and ultraviolet–visible determination revealed that the micelles had hydrodynamic diameters (D_h) below 200 nm, critical micelle concentrations from 50 to 55 mg/L, ζ potentials from -7 to -19 mV, and cloud points (CPs) of 34–36°C, depending on the [Monomer]/[Macroinitiator] ratios. The CPs and ζ potential absolute values were slightly decreased in simulated physiological media, whereas D_h increased somewhat. The hydrophobic camptothecin (CPT) was entrapped in polymer micelles to investigate the thermo-induced drug release. The stability of the CPT-loaded micelles was evaluated by changes in the CPT contents loaded in the micelles and micellar sizes. The MTT cell viability was used to validate the biocompatibility of the developed copolymer micelle aggregates. © 2013 Wiley Periodicals, Inc. J. Appl. Polym. Sci. 130: 4137–4146, 2013

KEYWORDS: copolymers; micelles; properties and characterization; self-assembly; stimuli-sensitive polymers

Received 2 January 2013; accepted 10 May 2013; Published online 12 July 2013
DOI: 10.1002/app.39530

INTRODUCTION

Block copolymers have attracted significant scientific and economic interest over the past few decades because of their ability to self-assemble into highly ordered core–shell nanoleveled micelle aggregates.[1,2] Reiss,[1] Alexandridis and Hatton,[3] Tuzar,[4] Eisenberg et al.,[5] Kakizawa and Kataoka,[6] Kabanov et al.,[7] Kataoka et al.,[8] and Kwon et al.,[9] as precursors in this field, have made outstanding contributions to shaping the block copolymer field. At present, the self-assembled micelle has become an up-and-coming drug carrier in the solubilization of hydrophobic anticancer drugs and the administration of controlled release drugs and targeted drugs. Poly(*N*-isopropyl acrylamide) (PNIPAM) is an extensively researched thermosensitive polymer drug carrier, which can undergo a sharp phase transition at the so-called lower critical solution temperature (LCST) of 32–33°C in aqueous media.[9] Various block copolymers containing PNIPAM fragments have been synthesized for biomedical applications.[10–13] This thermal response can be used to modulate the interactions of the micelles with cells, protein, and other biocomponents, and these copolymers are thus suitable for applications in the medicinal field as carriers of therapeutic and diagnostic drugs and can achieve peculiar targeting in tumor remedies.[14] Poly(lactic acid) (PLA) is frequently used as a structural motif for the hydrophobic components of block copolymers because of its good biocompatibility and applicable biodegradability. The combination of both PNIPAM and PLA is expected to result in an important biomedical material, where the PNIPAM segments as hydrophilic outer shells provide their structural stability and water solubility in aqueous solution and the PLA segments as hydrophobic inner cores can incorporate a large amount of hydrophobic drug. The copolymer micelles can deliver therapeutics via a stimuli-responsive targeting process by local heating to particular tissues, such as solid tumor sites.

Linear PNIPAM-*b*-PLA block copolymers have been studied extensively;[11–13] they have almost the same LCST values as the PNIPAM homopolymer. Their spontaneous self-assembly in aqueous solution and their drug loading and release depends on the media temperature, copolymer compositions, PLA and PNIPAM block lengths, hydrophobic interactions among the PNIPAM chains, intermolecular hydrogen bonding between the

Applied Polymer SCIENCE

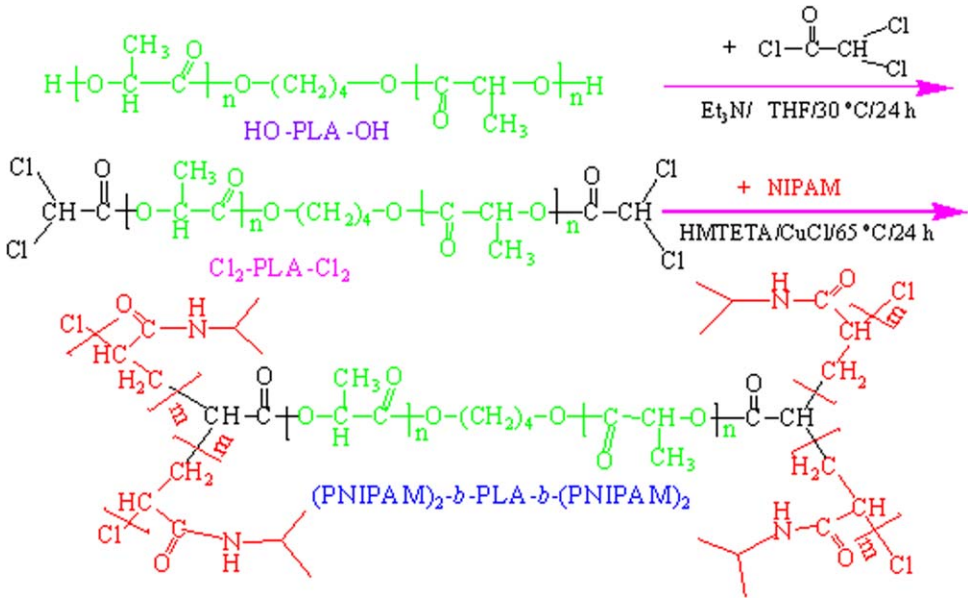

Scheme 1. Representative scheme of the synthesis of the A_2BA_2-type $(PNIPAM)_2$-*b*-PLA-*b*-$(PNIPAM)_2$ block copolymers. [Color figure can be viewed in the online issue, which is available at wileyonlinelibrary.com.]

PNIPAM chains and water molecules, and intramolecular hydrogen bonding between the $-CONH_2$ groups. With advances in polymer synthesis techniques, some well-defined copolymers with complex architectures, such as brush, comb, star (Y and H type, etc.), hyperbranched, and dendrimer types, can be readily prepared.[14–18] These copolymers with unique architectures exhibit special microphase separation structures both in the bulk and in solution mainly because (multi)blocks are stretched from a single junction; this has an important influence on the self-assembly micellization and stimuli-responsive properties.[19] In particular, (H or four-armed) star block copolymers have a unique space configuration, and their low viscosity, small radius of gyration, and hydrodynamic volume make their degradation products completely drain out of the body. Hence, they do not cause any accumulation and long-term side effects in the body. Compared with linear analogues, H or four-armed type block copolymers generally have a higher drug loading capacity (LC) and encapsulation efficiency and more sustained drug release because of their loosely packed cores and stronger interactions between hydrophobic blocks and drug molecules endowed by their unique architecture.[11] Therefore, it is necessary to elaborately design and develop a block copolymer with a novel H or four-armed star structure to provide it with a special microphase separation structure to tune the stimuli-triggered micellization behavior to improve the micelle stability and drug loading and release. Furthermore, the effects of the architecture on the fundamental parameters of the micelles, the micellization process, and the drug loading and release need to be elucidated. Such studies will help in the understanding of the fundamental principles governing the self-organization of block copolymers into micelles; this in turn will provide guidelines for designing polymer molecules for specific drug-release applications.

Recently, we achieved an unexpected reaction on a dichloroacetyl chloride ($CHCl_2COCl$), which showed us an easy way to synthesize A_2BA_2 star block copolymers. This unique architecture may have important effects on the static and dynamic stability, morphology, size, and size distribution of the micelles and may further affect the performance of the micelles, including the drug loading and release rate and even the *in vivo* circulation and distribution. Because of its good biocompatibility and biodegradation of PLA, we used it as hydrophobic blocks in the block copolymers. We anticipated that new thermoresponsive A_2BA_2-type block copolymers could be achieved through the combination of PNIPAM with PLA via atom transfer radical polymerization (ATRP), and their thermosensitive self-assembly micellization behavior in aqueous solution was examined by the modulation of the feed ratios and the medium temperature. Moreover, the *in vitro* cytotoxicity was valued, and the drug-loading and drug-release profiles with hydrophobic camptothecin (CPT; an anticancer drug) as a model drug were investigated to validate possibility of using the as-prepared copolymer micelles as a drug-delivery system.

EXPERIMENTAL

Materials and Reagents

Hydroxyl-terminated poly(lactic acid) (HO–PLA–OH), with a molecular weight (MW) of 3000 (degree of polymerization = 33), was purchased from Jinan Daigang Biomaterial Co., Ltd. (China). Dichloroacetyl chloride (purity > 98.0%) was supplied by TCI, Shanghai Corp., without further purification. Tetrahydrofuran (THF; purity > 99.0%) and triethylamine (TEA or Et_3N) were provided by Sinopharm Chemical Reagent Co., Ltd., and were dried over CaH_2 and distilled before use. *N*-Isopropylacrylamide (NIPAM; 98%), and cuprous chloride (CuCl; 99.95%) were supplied by the Aladdin Corp. and were used as received. 1,1,4,7,10,10-Hexamethyltriethylenetetramine

(HMTETA; 97%) was from Sigma-Aldrich. Isopropyl alcohol and dimethyl sulfoxide (DMSO; analytical grade) were obtained from the Fuchen Chemical Reagent Factory (Tianjin, China). All other chemicals were analytical grade and were used as received.

Experimental Procedures

The synthesis of the A_2BA_2-type $(PNIPAM)_2$-*b*-PLA_{33}-*b*-$(PNIPAM)_2$ block copolymers was achieved via the following two-step reaction, as shown in Scheme 1.

Chloropolyactic acid (Cl_2–PLA–Cl_2) was prepared by an HO–PLA–OH esterification reaction with dichloroacetyl chloride. Specifically, 2 g (0.67 mmol) of HO–PLA–OH and 0.28 mL (ca. 2.08 mmol) of TEA were dissolved in 15 mL of dried THF in a dried, three-necked flask with full stirring. Then, the solution was cooled to 0°C, and 0.20 mL of dichloroacetyl chloride (ca. 2.08 mmol) dissolved in advance in about 5 mL of THF was added dropwise to the solution with a constant-pressure funnel within 30 min (1–2 drops/min) under the protection of nitrogen gas. The reaction mixture was kept at 0°C for 2 h with stirring, and then the reaction proceeded at room temperature for 24 h. The resulting solution was filtered by a Buchner funnel, and the solvent was evaporated to around 5–10 mL with a rotary evaporation apparatus, and a viscous fluid was obtained. After the viscous fluid was recrystallized in eightfold cold diethyl ether, and then suction filtration was carried out, and white crude products were obtained. The resulting Cl_2–PLA–Cl_2 was achieved by the drying of the crystals *in vacuo* at 25°C, and the product was confirmed by ^{1}H-NMR spectroscopy.

The $(PNIPAM)_2$-*b*-PLA_{33}-*b*-$(PNIPAM)_2$ copolymers were synthesized by an ATRP route, as shown in Scheme 1. The reaction were conducted in a Schlenk tube at [Cl_2–PLA–Cl_2]/[CuCl]/HMTETA/[NIPAM] molar ratios of 1:7:8:200 and 1:7:8:400 in 4 mL of a DMSO/isopropyl alcohol (1:1 v/v) mixed solvent. Before the polymerization reaction, three consecutive standard freeze–pump–thaw cycles were performed to exclude oxygen from the polymerization solution. The polymerization tube was sealed and placed in a 65°C water bath, and the reaction was allowed to proceed for 24 h with stirring. The vial was quenched, and the reaction mixture was diluted with THF. The diluted mixture was passed through a neutral Al_2O_3 column to remove the copper complex. After most of the THF was removed by rotary evaporation, the crude polymer solution was placed in a dialysis bag with a molecular weight cutoff (MWCO) of 5000 (Spectrum Laboratories, Inc.) for dialysis against 1000 mL of distilled water at room temperature for 1 week. The water was replaced hourly for the first 3 h and then once every 8 h. The resulting products were dried in a vacuum oven at room temperature until a constant weight was reached (yield = 46%).

Preparation of the $(PNIPAM)_2$-*b*-PLA_{33}-*b*-$(PNIPAM)_2$ Micelle Aggregates

A dialysis method was used to prepare the $(PNIPAM)_2$-*b*-PLA_{33}-*b*-$(PNIPAM)_2$ micelle aggregates. Concretely, 25 mg of each copolymer powder was dissolved in 8 mL of dimethylformamide (DMF) at room temperature with stirring. The solution was put into a dialysis bag with a MWCO of 5000 and dialyzed against 1000 mL of deionized water at room temperature for 2 days with vigorous stirring. The water was replaced overnight and, in particular, was changed once per hour in the first 3 h. The micellar solution was diluted with deionized water to the desired concentration for further measurements.

Characterization and Measurements

An AVATAR 360 ESP Fourier transform infrared (FTIR) spectrometer (Nicolet) was used to characterize structure of the copolymers, and the samples were pressed into KBr pellets. ^{1}H-NMR was further used to determine the chemical compositions of the copolymers on a 300-MHz Bruker Avance NMR spectrometer (Bruker, Germany) with $CDCl_3$ as a solvent at 25°C, and TMS was used as an internal standard. The MW and polydispersity index (PDI) of the copolymers were determined by size exclusion chromatography (SEC; EcoSEC, Tosoh Corp., Japan) in THF as the eluent at a flow rate of 1.0 mL/min at a column temperature of 35°C; the setup consisted of a Tosoh isocratic pump with a parallel liquid supply, a Tosoh Brice-type, double-path, double-flow refractive-index detector, and two TSKgel SuperMultiporeHZ-M columns (6 × 150 mm). The previous solution was filtered through a 0.45-μm polytetrafluoroethylene syringe filter before the measurement. The SEC setup was calibrated with low-polydispersity polystyrene standards (PStQuickMP-M, Tosoh Corp., Japan).

The critical micelle concentration (cmc) of the copolymer micelle aggregates in aqueous solutions was determined by means of the surface tension technique on a DCAT21-tenometer (DataPhysics, Germany) with the Wilhelmy plate method. In brief, 40 mL of a series of the copolymer solutions containing different concentrations from 1×10^{-1} to 5×10^{-5} mg/L was prepared, and the sample solutions were left overnight to equilibrate at room temperature. The cmc value was evaluated from plots of the static surface tension versus the logarithm of the concentration. An ultraviolet–visible (UV–vis) spectrophotometer (U-3900, Hitachi, Japan) was used to examine the phase-transition temperature, namely, the cloud point (CP) or LCST of the copolymer micelle solution, which was acquired at the temperature with half of the optical transmittance between below and above the transition; the wavelength was fixed at 500 nm.

The morphology and size of the copolymer micelle aggregates were observed with a JEM-2100 transmission electron microscope (Electronics Corp., Japan). The transmission electron microscopy (TEM) images were obtained at an accelerating voltage of 200 keV, and we prepared the sample by dipping a drop of the micelle dispersion on a copper grid with carbon film. Excess copolymer solution was wiped off with filter paper, and the grid was dried under an ambient atmosphere for 1 h. It was necessary to stain the sample with 2% phosphotungstic acid solution for contrast before the measurement. A laser particle size–ζ potentiometer (Delsa Nano C, Beckman Coulter) was used to evaluate the hydrodynamic diameters (D_h) and ζ potential values of the block copolymer micelle aggregates. All of the sample measurements were performed at 25°C.

Loading of CPT and Release from the Copolymer Micelles

CPT was used as a model drug to evaluate the drug loading and release from the as-prepared copolymer micelles, and

experiments were carried with reference to the study reported by Li et al.[20] Specifically, 30 mg of copolymer sample and 5 mg of CPT were dissolved in 5 mL of DMF, and then the solution was transferred into a dialysis bag (MWCO = 5000 Da) to dialyze against 1000 mL of deionized water for 24 h to remove the free CPT. The dialysate was dried by lyophilization and weighed. The drug LC and entrapment efficiency (EE) were estimated by the following equations:

$$\text{LC}\,(\%) = (\text{Mass of CPT in the micelles}/\text{Mass of copolymer in the formulation}) \times 100\% \quad (1)$$

$$\text{EE}\,(\%) = (\text{Mass of CPT in the micelles}/\text{Mass of CPT in the initial solution}) \times 100\% \quad (2)$$

The CPT concentration was determined with a UV–vis spectrometer (U-3900/3900H, Titachi Corp., Japan) at a wavelength of 366 nm. The standard calibration curve was obtained from the linear relationship between the UV absorbance and the CPT concentration in DMF.

Next, 5 mg of the lyophilized CPT-loaded sample was dissolved in 10 mL of phosphate-buffered saline (PBS) at pH 7.4 and then immediately diverted into a dialysis bag against 1000 mL of PBS at pH 7.4 and a temperature 25 or 39°C. Aliquots of 4 mL of dialysate were taken from the beaker periodically and measured by the UV–vis spectrophotometer at 366 nm to acquire the amount of CPT released through the bag. The samples were returned to the receiver solution after measurement. The cumulative CPT release (%) was calculated on the basis of the following formula:

$$\text{Cumulative drug release}\,(\%) = M_t/M_0 \times 100 \quad (3)$$

where M_t is the amount of CPT release from micelles at time t and M_0 is the amount of CPT loaded in the copolymer nanoscale micelles.

In Vitro Biocompatibility Valuation

MTT assay was adopted to evaluate the *in vitro* cytotoxicity or biocompatibility against L929 mouse embryonic fibroblasts, which was performed according to our previous study.[21] Before the assay, cells were seeded into a 96-well plate at a density of 1×10^4 cells per well, cultured overnight, and then incubated with blank and CPT-loaded polymer micelles in a complete Dulbecco's modified eagle's medium (DMEM) containing 10% hyclone fetal bovine serum (high-glucose DMEM) at 37°C in a 5% CO_2 atmosphere for 24 h. Then, the culture medium was removed and replaced with 100 μL of the medium containing the previous polymer micelles. After 72 h of culturing, the medium was replaced with 100 μL of fresh DMEM; this was followed by the addition of 25 μL of MTT stock solution to the fibroblasts. After 4 h of incubation, the supernatant was discarded, and then 150 μL of DMSO was added; the mixture was shaken for 10 min at room temperature. For reference purposes, cells were seeded in a fresh culture medium (negative control) under the same conditions. Each assay was performed four times. The optical density with polymer micelles (OD_{sample}) and the optical density without polymer micelles ($OD_{control}$) were measured by a 96-well universal microplate reader (model 680, Bio-Rad Laboratories, Ltd., United Kingdom) with a wavelength of 490 nm, and the cell viability was calculated with the following equation:

$$\text{Cell viability}\,(\%) = \left(\text{OD}_{\text{sample}}/\text{OD}_{\text{control}}\right) \times 100\% \quad (4)$$

In this assay, the Student's test was used to determine the significance of any pairs of observed differences. The differences were considered statistically significant at $p < 0.05$. All quantitative results are reported as the mean values plus or minus the standard deviations.

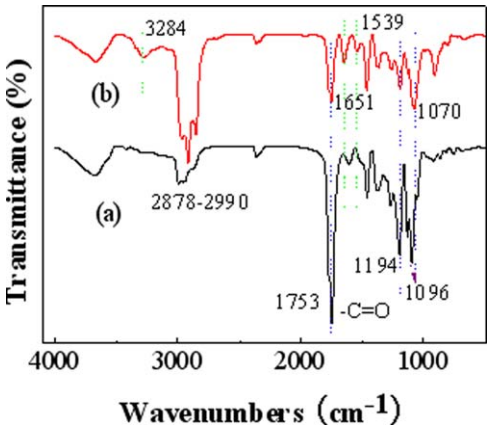

Figure 1. FTIR spectra of (a) Cl_2–PLA–Cl_2 and (b) $(PNIPAM)_2$-*b*-PLA-*b*-$(PNIPAM)_2$. [Color figure can be viewed in the online issue, which is available at wileyonlinelibrary.com.]

Stability of the CPT-Loaded Copolymer Micelles

The drug-loaded micelles were stored in a dark place (the refrigerator) at 9°C for 1 month. The stability was monitored by changes in the CPT concentration and particle size during the storage period as described previously.

RESULTS AND DISCUSSION

Synthesis and Structural Characterization

Figure 1 shows the FTIR spectra of the $(PNIPAM)_2$-*b*-PLA_{33}-*b*-$(PNIPAM)_2$ block copolymer and its initiator. It was clear that Cl_2–PLA–Cl_2 [Figure 1(a)] produced characteristic vibration peaks at 1753 cm^{-1}, which was assigned to the ester carbonyl stretching mode; 1096–1191 cm^{-1}, which was attributed to —C—O—C— stretching; and 2878–2990 cm^{-1}, which belonged to alkyl vibrations. In Figure 1(b), the newly appearing vibration peaks at 3284, 1651, and 1539 cm^{-1} were ascribed to —N—H— stretching, amido–carbonyl stretching (amide), and —N—H— bending modes, which were typical amide characteristics. These results preliminarily indicated that $(PNIPAM)_2$-*b*-PLA_{33}-*b*-$(PNIPAM)_2$ was successfully synthesized through ATRP.

The ^{1}H-NMR spectra were further used to confirm the chemical structure of the copolymer, as displayed in Figure 2(a,b). The initiator Cl_2–PLA–Cl_2 produced three distinct signals [Figure 2(a)] at about 5.90 ppm, which was ascribed to the methylidyne proton signal of the initiator residues (*s*, 2H, —OOC*CH*Cl_2); 5.10 ppm, which was attributable to the methylidyne protons [*q*, 33H, —OOC*CH*(CH_3)O—] in the PLA blocks; and 1.50 ppm, which was associated with the methane protons [*d*, 100H, —OOCCH(*CH_3*)O—]; this signal was strong and superposed on the methylene protons of the butanediol residues [*t*, 4H,

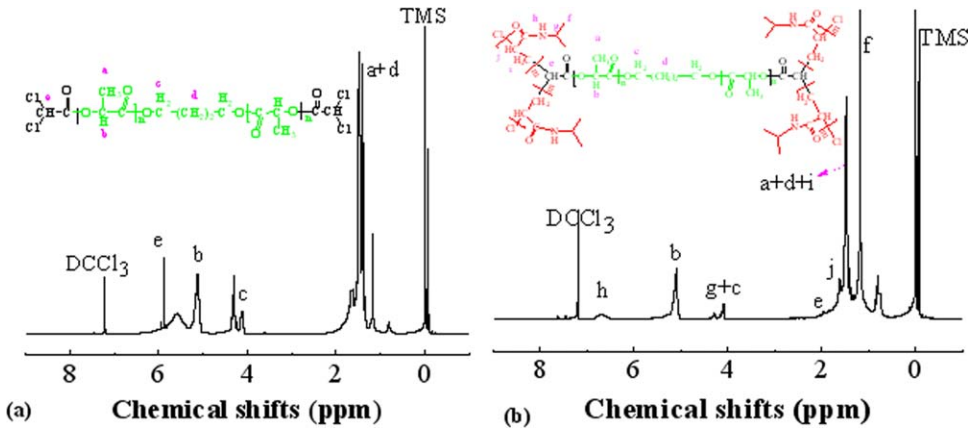

Figure 2. ^{1}H-NMR of (a) Cl_2–PLA–Cl_2 and (b) $(NIPAM)_2$-*b*-PLA_{33}-*b*-$(PNIPAM)_2$ in $CDCl_3$ ($DCCl_3$ = deuteriochloroform). [Color figure can be viewed in the online issue, which is available at wileyonlinelibrary.com.]

—$OOCCH_2(CH_2)_2CH_2COO$—]. In addition, the other methylene protons of the butanediol residues connected with ester carbonyl groups and appeared at about 4.10 ppm [*t*, 4H, —$OOCCH_2(CH_2)_2CH_2COO$—]. These results indicate that the macroinitiator was successfully prepared by an esterification reaction avenue. In the ^{1}H-NMR spectra of the resulting $(PNIPAM)_2$-*b*-PLA_{33}-*b*-$(PNIPAM)_2$ block copolymer [Figure 2(b)], all of the shifting signals from Cl_2–PLA–Cl_2 appeared at almost the same positions, except the methylidyne proton signal of the initiator residues at about 1.97 ppm, which was due to the linkage group from chlorine atoms (—$OOCCHCl_2$) to the methylene protons [—$OOCCH(CH_2)_2$—]. In addition, the chemical shift signals reflecting the PNIPAM structural characteristics appearing at $\delta = 1.20$ ppm were attributable to the methyl protons [*br, d,* —$CH(CH_3)_2$], and those around $\delta = 4.08$–4.10 ppm were ascribed to characteristic signals of methylidyne protons [br, *m*, —$CH(CH_3)_2$ in the PNIPAM blocks]; this overlapped with d signals; 1.65 ppm, which was assigned to the hydrogen protons of methylidyne (br, —CH—CH_2—); 1.50 ppm, which was ascribed to methylene protons (br, —CH—CH_2—); and 6.72 ppm, which corresponded to the characteristic signal of hydrogen protons of the imido group (—NH—C═O) in the PNIPAM moieties. The ^{1}H-NMR results further corroborate the synthesis of the poly(*N*-isopropyl acrylamide)$_2$-*b*-poly(lactic acid)-*b*-poly(*N*-isopropyl acrylamide)$_2$ [$(PNIPAM)_2$-*b*-PLA-*b*-$(PNIPAM)_2$] block copolymers.

SEC measurements were carried out to obtain information on the MWs and PDIs of the block copolymers, as shown in Table I, which also lists the detailed formulas and conditions and the sample codes. As shown in Table I, the MWs of the copolymers were enhanced with increasing [Monomer]/[Initiator] molar ratios, with number-average molecular weights (M_ns) from 1.05 $\times$ 10^4 to 1.24 $\times$ 10^4 and PDIs below 1.11; this reflected the features of the controlled free-radical polymerization of the NIPAM monomer initiated by the macroinitiator Cl_2–PLA–Cl_2 during the ATRP synthesis. The narrower MW distribution further hinted that there was no residual NIPAM monomer and Cl_2–PLA–Cl_2 left after the ATRP polymerization reaction and dialysis. From the M_n values of the resulting polymer acquired by SEC, we deduced the number of NIPAM units attached to the Cl_2–PLA–Cl_2 initiator, as shown in Table I.

cmc Determination and Thermotriggered Response

The A_2BA_2-type thermosensitive amphiphilic block copolymers consisting of hydrophilic PNIPAM blocks and hydrophobic PLA segments synthesized in this study could self-assemble into micelles with a core–shell architecture in aqueous solutions. To examine the micellization behavior of the block copolymers, cmc, as a measure describing the physical properties of the micelle, was examined by surface tension techniques, as depicted in Figure 3. From the place where an obvious turning point occurred in the surface tension versus the solution concentration curve, it was easy to determine the cmc concentration. In the case of the two block copolymers, their cmc values were about 57.0 and 52.3 mg/L; these values corresponded to [Initiator]/[NIPAM] molar ratios of 1:200 and 1:400, respectively. Although the cmc difference was very small, the values decreased slightly with increasing NIPAM content. The low cmc value suggested that the block copolymer with a suitable chain length was more stable in the aqueous solution and that the block copolymer micelle aggregates may be stable enough to withstand intravenous injection into a large volume of blood. cmc is not the only factor that influences the stability of a

Table I. Formulations, Codes, and SEC Data for the Different Block Copolymers

Copolymer	$[Cl_2$-PLA-$Cl_2]$/[NIPAM][a]	$M_n \times 10^4$	$M_w \times 10^4$	PDI
$PNIPAM_{23})_2$-*b*-PLA_{33}-*b*-$(PNIPAM_{23})_2$	1:200	1.05	1.15	1.09
$(PNIPAM_{27})_2$-*b*-PLA_{33}-*b*-$(PNIPAM_{27})_2$	1:400	1.24	1.38	1.11

M_w, weight-average molecular weight.
[a] Molar ratio of the initiator to NIPAM.

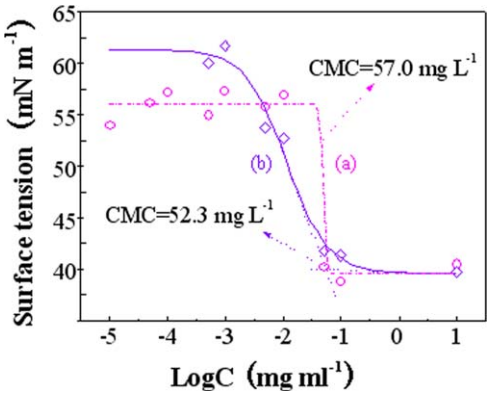

Figure 3. Surface tension dependence on the logarithms of the $(PNIPAM)_2$-*b*-PLA_{33}-*b*-$(PNIPAM)_2$ copolymer concentrations (*C*s) at room temperature with different Cl_2–PLA–Cl_2/NIPAM molar ratios: (a) 1:200 and (b) 1:400. [Color figure can be viewed in the online issue, which is available at wileyonlinelibrary.com.]

micelle. The glass-transition temperature, hydrophobic–hydrophilic block ratio, ζ potential, and conjugated drug content also affect the thermodynamic and kinetic stability of micelles.[5] Consequently, a comprehensive analysis should fully be taken into account before a conclusion on the micellar stability is made. Further examination of the stability in this study was conducted through ζ-potential analysis.

With the thermotriggered response of the PNIPAM polymers, which had LCSTs or CPs of about 32°C, the temperature-sensitive phase transitions of the as-synthesized block copolymers in aqueous solution and simulated physiological media were investigated by transmittance determination at various temperatures, as displayed in Figure 4. It is clear from Figure 4(a) that these copolymers had a very close but slightly decreased CP values of about 35.5 and 34.4°C in aqueous solution; these values corresponded to [Cl_2–PLA–Cl_2]/[NIPAM] molar ratios of 1:200 and 1:400, respectively. Meanwhile, we noticed that the copolymer with a low NIPAM ratio had a transmittance of only about 35% or so below CP, whereas the copolymer with a high NIPAM ratio bore a higher transmittance. This suggested that the former was more ready to form micelle aggregates below CP because of the relatively high hydrophobic/hydrophilic chain (PLA/PNIPAM) length ratios. However, the transmittance of the copolymer with a high NIPAM ratio more remarkably decreased in aqueous solution than that with a low NIPAM ratio. The probability was that the longer PNIPAM coronas induced stronger hydrophobic transition or collapse and thus a more remarkable phase transition. The copolymers were more readily to assemble into stable thermotriggered micelles. Plunkett et al.[22] once examined the PNIPAM chain collapse dependence on the MW and grafting density and found that chain collapse occurred at high MWs or chain lengths, as expected. The extent of the change in PNIPAM at the transition temperature depended on the MW. This was in good agreement with our previous analysis and thus clearly explained why there was such a difference in the transmittance and CPs between the two polymers with ratios of 1:200 and 1:400. With the small MW difference taken into account, their CPs had little diversity. The same transmittance change was also found in the PBS solutions at pH 7.4, as shown in Figure 4(b), and the CP values were about 33.9 and 33.3°C; these values corresponded to [Cl_2–PLA–Cl_2]/[NIPAM] molar ratios of 1:200 and 1:400, respectively. Likewise, the reason that the high NIPAM molar ratio produced a slightly low CP was that longer thermosensitive NIPAM chains existing in the composition of the block copolymers resulted in more sensitive temperature responsivity, as described previously. The small difference in CP in both aqueous solution and simulated physiological ambient conditions indicated that the [Cl_2–PLA–Cl_2]/[NIPAM] molar ratios had some effect on the CP values more or less, and the CP values depended on the composition of block copolymers to some extent, especially the MWs or chain lengths of the PNIPAM blocks. Compared with the CP data in aqueous solution, the lowered CP values in the PBS solution at pH 7.4 may have been related to the salting-out effect of salt ions existing in the buffered solutions. It was the existence of these ions that influenced the thermosensitive micellization behavior and induced slightly lowered CP values; this was proven by the studies of Chang et al.[23] and Hoffman and Park.[24] In fact, the introduction of the salts with high ionic strength resulted in strong ionic hydration and thus weakened, or even destroyed, the

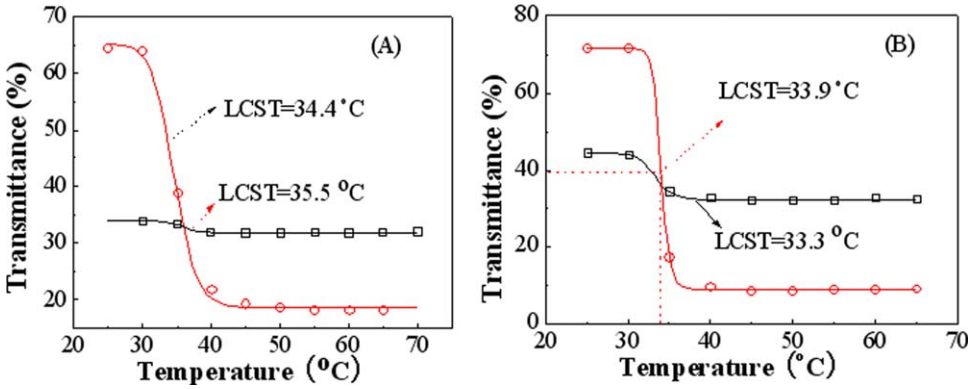

Figure 4. Transmittance change of the thermosensitive $(PNIPAM)_2$-*b*-PLA_{33}-*b*-$(PNIPAM)_2$ block copolymers with different Cl_2–PLA–Cl_2/NIPAM molar ratios: (□) 1:200 and (○) 1:400 at $\lambda = 500$ nm by UV–vis spectroscopy in (A) aqueous solution and (B) PBS solution at pH 7.4 with temperature (250 mg/L). [Color figure can be viewed in the online issue, which is available at wileyonlinelibrary.com.]

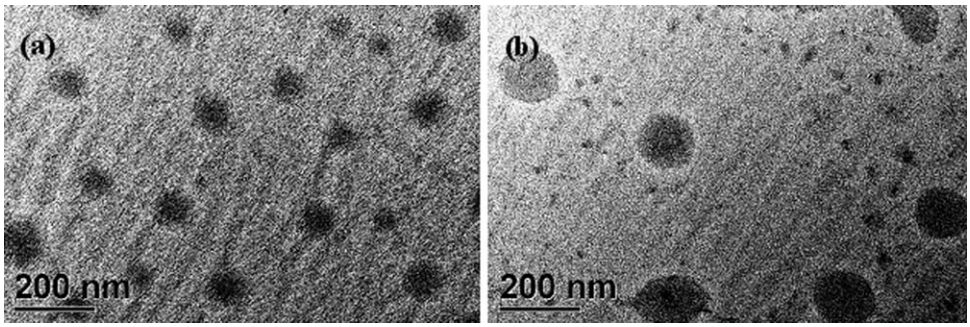

Figure 5. TEM images of the representative $(PNIPAM_{27})_2$-*b*-PLA_{33}-*b*-$(PNIPAM_{27})_2$ block copolymer micelle aggregates (concentration = 250 mg/L) in (a) aqueous solution and (b) pH 7.4 PBS solution.

(hydrogen-bonding) interactions between the water molecules and PNIPAM chains as shell layers of micelle stabilization; this induced changes in the soluble–insoluble properties of the nonionic PNIPAM solutions. Meanwhile, the disruption of the interactions between the water and PNIPAM chains in return induced the PNIPAM–PNIPAM interactions. These interactions were equivalent to an increase in the hydrophobicity of the PNIPAM chains; this made the CP value of the copolymer micelles shift to a slightly lower temperature.

Morphologies and Sizes of the Block Copolymer Micelle Aggregates

Figure 5 displays TEM photographs of the synthesized $(PNIPAM_{27})_2$-*b*-PLA_{33}-*b*-$(PNIPAM_{27})_2$ four-armed star-shaped block copolymer micellar aggregates in different media. Obviously, the copolymer micellar aggregates presented a regular spherical appearance and a well-defined size distribution whether they were in aqueous solution or in a simulated physiological environment (PBS solution at pH 7.4). The micelle aggregates had an average particle diameter of approximately 78–85 nm in aqueous solution and about 130 nm in PBS solution at pH 7.4. This size conforms to the requirements for endocytosis entering into cells, and thus transfection cloning achieves success.[16] Table II tabulates the D_h and PDI values of the block copolymers with different composition ratios. As shown in Table II, D_h increased both in the aqueous solution and in PBS solution at pH 7.4 with increasing [NIPAM]/[Cl_2–PLA–Cl_2] molar ratio, probably because of the longer PNIPAM hydrophilic chains. On the other hand, we noticed that these copolymer micelle aggregates produced higher D_h values in PBS solution at pH 7.4 than in aqueous solution and exhibited similar changes to the TEM diameters. The increased particle size in PBS was perhaps due to further aggregation, which resulted from the screening of the charge present in media. Kakizawa and Kataoka[6] reported that a polyion complex with small ζ potentials formed insoluble large aggregates at the charge-neutralized mixing ratio because of the hydrophobic nature of the associates; this may have been responsible for the large micelle aggregates when we considered the close neutral conditions used in this study. The larger D_h may have made up for the enhancement of the loading amount of the drug. The D_h range of the block copolymer micelle aggregates were typically in the range from 130 to 240 nm in the two media, and the size distributions or PDIs were significantly narrow (<0.27), with a well-defined size monodispersity. Therefore, they not only could prevent premature elimination via glomerular filtration in the kidneys or make them less susceptible to clearance by the reticuloendothelial system but could also enter blood vessels and capitalize on the enhanced permeation and retention effect for passive accumulation in the target lesion tissues;[25] this is very significant for drug controlled release applications.

Physicochemical Characteristics of the Block Copolymer Micelle Aggregates

The physicochemical characteristics of the block copolymer micelles were related to the *in vivo* and *in vitro* fate of the block copolymer micelles. The ζ potential is an essential parameter that is correlated with the stability of colloidal dispersions and affects the interaction with biological entities, such as proteins and cell membranes, which results in the modulation of the pharmacokinetics of the particles and their uptake into cells.[16] Therefore, it was necessary to analyze the surface properties of the as-prepared block copolymer micelle nanoparticles through measurement of the ζ potentials and further to verify the

Table II. D_h Values, PDIs, and ζ Potentials of the Synthesized Block Copolymers in Various Media at Room Temperature

Sample[a]		$D_h \pm$ SD (nm)	PDI ± SD	ζ potential (mV)
1:200	Aqueous solution	133.81 ± 3.96	0.2453 ± 0.0124	−16.71 ± 2.01
	PBS of pH 7.4	175.35 ± 6.98	0.2280 ± 0.0102	−5.28 ± 0.41
1:400	Aqueous solution	160.18 ± 30.29	0.2683 ± 0.0234	−9.12 ± 1.71
	PBS of pH 7.4	234.81 ± 22.56	0.2163 ± 0.0186	−4.59 ± 1.36

Polymer concentration = 250 mg/L. SD, standard deviation.
[a] Molar ratio of the initiator to NIPAM.

micellar stability. Table II summaries the ζ potential data of the $(PNIPAM)_2$-*b*-PLA_{33}-*b*-$(PNIPAM)_2$ block copolymers with different [NIPAM]/[Cl_2–PLA–Cl_2] molar ratios in different media at room temperature. In both aqueous solution and PBS, the ζ potentials of the micelle aggregates became more negative with decreasing [NIPAM]/[Cl_2–PLA–Cl_2] molar ratios; this was consistent with the decreased MW of the copolymers shown in Table I. Taking into account the identical PLA MW, we observed that the PNIPAM chain lengths or MWs in copolymer compositions decreased; this in turn led to a relatively increased hydrophobic/hydrophilic chain (PLA/PNIPAM) length ratio. Thus, the hydrophilicity of the micelle aggregate surface decreased, whereas the hydrophobicity increased; this caused the ζ potentials to get more negative. Naha et al.[26] once found a similar change in the ζ potentials and proved the change in the hydrophilicity/hydrophobicity resulting from NIPAM/*N*-*tert*-butyl acrylamide ratios by contact angle measurements. We therefore concluded that it was easier for high-fractional hydrophobic compositions and short hydrophilic chains to form stable micellar nanoparticles. The negative ζ values may have been the result of negative charges absorbed on the surface of the micelle nanoparticles due to the existence of a contact potential between two materials with different permittivities in a way that the material with the lower dielectric constant carried the negative charge.[27] The ζ potential measurements in various media systems demonstrated that the ζ potentials in aqueous solution were more negative than those in PBS at pH 7.4; this indicated that the micelle aggregates could more stably exist in aqueous solution than in PBS at pH 7.4, and the salinity may have had some impact on the ζ potentials. Liu et al.[28] once investigated the effect of the NaCl concentration on the ζ potential and concluded that the electrostatic shielding was the dominant factor causing the decreased ζ potential absolute values at low salt concentrations. On the other hand, the ionic salts introduced here also resulted in strong ionic hydration; this weakened the interactions between water and PNIPAM and induced interactions between PNIPAM and PNIPAM. This increased the hydrophobicity of PNIPAM or hydrophobic isopropyl groups on the micelle surface, led to a slight flocculation of the nonionic PNIPAM copolymer micelles, and thus decreased the absolute values of the ζ potentials.[29]

Thermotriggered Drug Release

CPT, a natural plant alkaloid, has been shown to be a potent anticancer drug.[30] However, its water insolubility and lactone ring instability restrict its applications in cancer therapy. On the other hand, a drug should be targeted to the lesion sites and have little impact on the target organs, tissues, and cells; this would not only improve its curative effect but also reduce its side effects. If the core–shell morphologies of the copolymer micelles were taken into account, the hydrophobic internal nuclei could accommodate hydrophobic drug molecules and effectively protect the active lactone ring of CPT from hydrolysis, and the hydrophilic outer shells could hold the micelle stably in aqueous medium. CPT was encapsulated in the as-prepared block copolymer micelles. The LC and EE of CPT entrapped in the $(PNIPAM_{23})_2$-*b*-PLA_{33}-*b*-$(PNIPAM_{23})_2$ were 11.3 and 30.0%, respectively, and those of the CPT entrapped in the $(PNIPAM_{27})_2$-*b*-PLA_{33}-*b*-$(PNIPAM_{27})_2$ were 13.2 and 32.5%, respectively. The data suggest that the drug LC and EE of the copolymer micelles for hydrophobic drugs increased with increasing length or M_n of the PNIPAM blocks under identical lengths of hydrophobic blocks. The increased LC and EE may have been to the relatively small diffusion of CPT entrapped in the hydrophobic cores out of the copolymer micelles with properly long PNIPAM chains. This copolymer micelle may have well attained a proper copolymer–drug hydrophilic/hydrophobic balance on the basis of its highly hydrated shell and could thus encapsulate and keep the more water-insoluble CPT drug in the hydrophobic micelle cores to prevent more diffusion; this led to a slightly high CPT content and EE in the case of the identical hydrophobic interactions between the CPT and micelle cores.

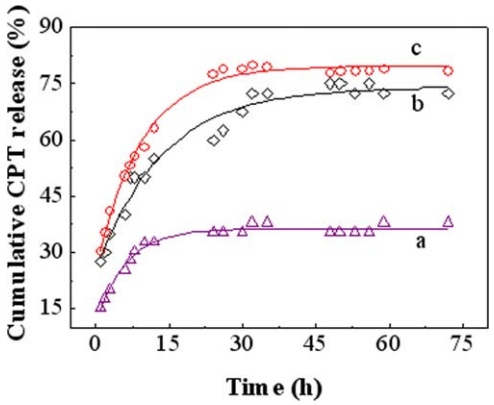

Figure 6. Cumulative release of CPT in PBS at pH 7.4 from the (a) $(PNIPAM_{27})_2$-*b*-PLA_{33}-*b*-$(PNIPAM_{27})_2$ micelles at 25°C, (b) $(PNIPAM_{23})_2$-*b*-PLA_{33}-*b*-$(PNIPAM_{23})_2$ micelles at 39°C, and (c) $(PNIPAM_{27})_2$-*b*-PLA_{33}-*b*-$(PNIPAM_{27})_2$ micelles at 39°C. [Color figure can be viewed in the online issue, which is available at wileyonlinelibrary.com.]

The drug-release profiles from these copolymer micelles in PBS solution at pH 7.4 at medium temperature were investigated, as shown in Figure 6. It was obvious that the *in vitro* release of CPT from these micelle nanoparticles was temperature-dependent. The cumulative CPT releases at 25°C (below CP) and 39°C (above CP) were about 33 and 64% after 12 h, respectively, and were finally up to about 38 and 80% after 72 h, respectively, for the $(PNIPAM_{27})_2$-*b*-PLA_{33}-*b*-$(PNIPAM_{27})_2$ micelles. The faster CPT release above CP than below CP was mainly due to temperature-induced micellar structural changes. We, therefore, deduced that the mechanism of drug release in the designed four-star copolymer micelles may have been controlled only by the Fickian diffusion below CP, whereas an abnormal diffusion mode was produced above CP; this was accompanied by a decrease in D_h because of the increased hydrophobicity of the PNIPAM blocks. The shell contraction originating from the decrease in D_h above CP made the hydrophobic CPT diffuse out of the micellar cores more quickly[20] and exhibit a thermotriggered CPT release behavior. We also observed that the thermo-induced CPT release was controllable with time and did not produce an initial burst effect. These findings reveal that the CPT-encapsulated copolymer micelles could retain a sustained and controlled drug release for a long time. In particular, this release behavior could minimize

systemic leakage of drugs before it reaches the target sites but swiftly deliver the drug to lesion tissues in response to environmental temperature changes; this would, therefore, reduce the drug toxicity or side effects to normal tissues and enhance the drug-targeting properties. This is very significant for the development of an intelligent drug-delivery system. In addition, the release rate of CPT from the $(PNIPAM_{27})_2$-*b*-PLA_{33}-*b*-$(PNIPAM_{27})_2$ micelles was faster than that from the $(PNIPAM_{23})_2$-*b*-PLA_{33}-*b*-$(PNIPAM_{23})_2$ micelles during the whole release; this may have been due to more deformation of the thermo-induced micellar structure. Consequently, CPT release from the as-prepared copolymer micelles could be tailor-made through the variation of the copolymer composition or the length or M_n of PNIPAM blocks as micellar shells with a stabilization function.

In Vitro Cytotoxicity and Stability of the CPT-Loaded Micelles

The balance between the drug loading and micelle stability is a critical factor in the optimization of micelle-based formulations. To validate the possible applicability of the as-prepared copolymer micelles as a drug controlled release system, a cytotoxicity assay and stability experiment of the drug-loaded micelles were performed. Figure 7 shows the cell viabilities after 72 h of incubation of the blank and CPT-loaded $(PNIPAM_{27})_2$-*b*-PLA_{33}-*b*-$(PNIPAM_{27})_2$ micelles in the concentration range of polymer micelles from 10 to 1000 mg/L. It was clear that there was no significant difference in the cell viabilities for the blank copolymer micelles ($p < 0.05$), and these copolymer micelles were less cytotoxic to the L929 cells below 1000 mg/L, with a cell viability of 91–102%. The cell viabilities of the CPT-loaded copolymer micelles were lower than those of the blank micelles; this suggested that they were a little more cytotoxic than the blank copolymer micelles within the whole concentration range. For all this, the cell survival percentage was over 82%. This slightly decreased cell viability was mainly attributable to some CPT *in vitro* release.[31] These *in vitro* cytotoxicity assays showed that the blank and drug-loaded copolymer micelles were biocompatible with L929 cells, and consequently, they could be practically regarded as a safe drug-delivery carrier.

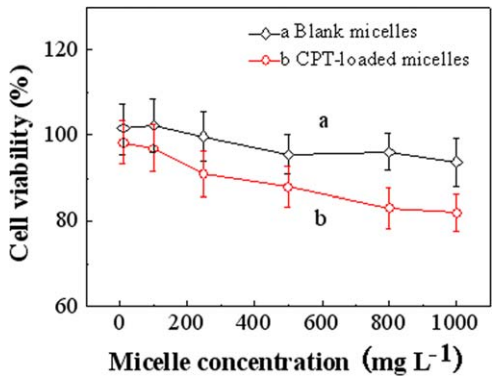

Figure 7. Cytotoxicity change in the (a) blank and (b) CPT-loaded $(PNIPAM_{27})_2$-*b*-PLA_{33}-*b*-$(PNIPAM_{27})_2$ micelles with concentrations from 10 to 1000 mg/L to L929 cells after 72 h of incubation as determined by MTT assay. [Color figure can be viewed in the online issue, which is available at wileyonlinelibrary.com.]

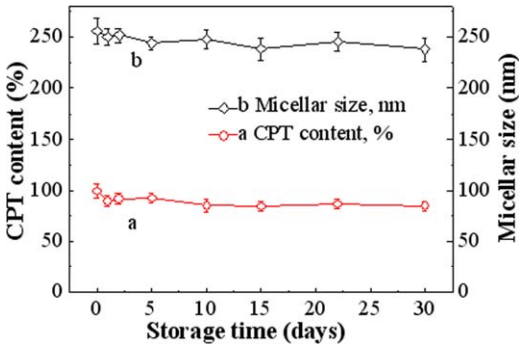

Figure 8. Changes in the (a) CPT concentrations loaded in the $(PNIPAM_{27})_2$-*b*-PLA_{33}-*b* -$(PNIPAM_{27})_2$ polymer micelle and (b) micellar nanoparticle sizes in PBS solution at pH 7.4 at 4°C after 30 days of storage. [Color figure can be viewed in the online issue, which is available at wileyonlinelibrary.com.]

Figure 8 displays the changes in the CPT concentrations loaded in the $(PNIPAM_{27})_2$-*b*-PLA_{33}-*b*-$(PNIPAM_{27})_2$ polymer micelles in PBS at pH 7.4 at 9°C as a function of the time. We noticed that the CPT-loaded micelles showed a loss of only about 8.91% CPT after 30 days without obvious observed CPT precipitation. The micelle solution remained in its original translucent or turbid state. The stability of the CPT-loaded micelles was also corroborated through changes in the micellar nanoparticle sizes measured by dynamic light scattering. As shown in Figure 8, the micelle nanoparticles had an average initial D_h size of 256.43 ± 12.93 nm. After 30 days of storage, the D_h size decreased slightly (ca. 237.99 ± 11.23 nm), presumably because of the release or decomposition of a small amount of CPT; there was only a 7.19% size change, and D_h remained practically unchanged. It should be noted that the initial D_h for the CPT-loaded micelles was larger than that for the blank micelles in PBS at pH 7.4 because CPT was entrapped into the core of the micelles. These findings suggest that the drug-loaded copolymer micelles had good long-term stability and could be included in a viable strategy for drug formulation and delivery. The micelle stability study at longer storage times is still ongoing.

CONCLUSIONS

In summary, novel A_2BA_2-type thermosensitive $(PNIPAM)_2$-*b*-PLA-*b*-$(PNIPAM)_2$ four-armed star block copolymers were successfully synthesized via ATRP with Cl_2–PLA–Cl_2 as a macroinitiator and NIPAM as a monomer; this was confirmed by FTIR, ^{1}H-NMR, and SEC measurements. The block copolymers could spontaneously assemble into thermotriggered nanosized core–shell micelle aggregates in aqueous solution, with cmc values from 52 to 57 mg/L, CPs or LCSTs from 33 to 36°C, and D_h values below 240 nm; this depended on the [Monomer]/[Macroinitiator] molar ratios and temperature. The CPT release from the as-prepared copolymer micelles exhibited thermotriggered release features, and the release was sustained and controlled and could be mediated through hydrophobic/hydrophilic components. The block copolymer micelles were biocompatible with L929 cells, and the CPT-loaded copolymer micelles had long-term stability. These findings strongly indicate that the block

copolymer micelles may practically be used as a safe and stable drug controlled release carrier.

ACKNOWLEDGMENTS

This work was supported by the Natural Science Foundation of China (contract grant sponsor NSFC 21273142), the Natural Science Foundation of Shaanxi Province (contract grant sponsor 2012JM6009), and the Graduate Education Innovation Funds (contract grant sponsor 2013CXS049).

REFERENCES

1. Riess, G. *Prog. Polym. Sci.* **2003**, *28*, 1107.
2. Gaucher, G.; Dufresne, M. H.; Sant, V. P.; Kang, N.; Maysinger, D.; Leroux, J. C. *J. Controlled Release* **2005**, *109*, 169.
3. Alexandridis, P.; Hatton, T. A. *Colloids Surf. A* **1995**, *96*, 1.
4. Tuzar, Z. J. *Macromol. Sci. Pure Appl. Chem.* **1992**, *29*, 173.
5. Allen, C.; Maysinger, D.; Eisenberg, A. *Colloids Surf. B* **1999**, *16*, 3.
6. Kakizawa, Y.; Kataoka, K. *Adv. Drug Delivery Rev.* **2002**, *54*, 203.
7. Kabanov, A. V.; Lemieux, P.; Vinogradov, S.; Alakhov, V. *Adv. Drug Delivery Rev.* **2002**, *54*, 223.
8. Kataoka, K.; Harada, A.; Nagasaki, Y. *Adv. Drug Delivery Rev.* **2001**, *47*, 113.
9. Kwon, G.; Naito, M.; Yokoyama, M.; Okano, T.; Sakurai, Y.; Kataoka, K. *Langmuir* **1993**, *9*, 945.
10. Wei, H.; Zhang, X. Z.; Chen, W. Q.; Cheng, S. X.; Zhuo, R. X. *J. Biomed. Mater. Res. Part A* **2007**, *83*, 980.
11. Wei, H.; Cheng, S. X.; Zhang, X. Z.; Zhuo, R. X. *Prog. Polym. Sci.* **2009**, *34*, 893.
12. Lo, C. L.; Lin, K. M.; Hsiue, G. H. *J. Controlled Release* **2005**, *104*, 477.
13. Xu, F.; Yan, T. T.; Luo, Y. L. *Macromol. Res.* **2011**, *19*, 1287.
14. Wan, X. J.; Liu, T.; Liu, S. Y. *Biomacromolecules* **2011**, *12*, 1146.
15. Zamurovic, M.; Christodoulou, S.; Vazaios, A.; Iatrou, E.; Pitsikalis, M.; Hadjichristidis, N. *Macromolecules* **2007**, *40*, 5835.
16. Cai, Y.; Tang, Y.; Armes, S. P. *Macromolecules* **2004**, *37*, 9728.
17. Li, L. Y.; He, W. D.; Li, W. T.; Zhang, K. R.; Pan, T. T.; Ding, Z. L.; Zhang, B. Y. *J. Polym. Sci. Part A: Polym. Chem.* **2010**, *48*, 5018.
18. Meyer, N.; Delaite, C.; Hurtrez, G.; Dumas, P. *Polymer* **2002**, *43*, 7133.
19. Tang, P.; Qiu, F.; Zhang, H. D.; Yang, Y. L. *J. Phys. Chem. B* **2004**, *108*, 8434.
20. Li, G.; Guo, L.; Ma, S. *J. Appl. Polym. Sci.* **2009**, *113*, 1364.
21. Xu, F.; Yan, T. T.; Luo, Y. L. *J. Bioact. Compat. Polym.* **2013**, *28*, 66.
22. Plunkett, K. N.; Zhu, X.; Moore, J. S.; Leckband, D. E. *Langmuir* **2006**, *22*, 4259.
23. Chang, Y.; Chen, W. Y.; Yandi, W.; Shih, Y. J.; Chu, W. L.; Liu, Y. L.; Chu, C. W.; Ruaan, R. C.; Higuchi, A. *Biomacromolecules* **2009**, *10*, 2092.
24. Park, T. G.; Hoffman, A. S. *Macromolecules* **1993**, *26*, 5045.
25. Ebrahim Attia, A. B.; Ong, Z. Y.; Hedrick, J. L.; Lee, P. P.; Ee, P. L. R.; Hammond, P. T.; Yang, Y. Y. *Curr. Opin. Colloid Interface Sci.* **2011**, *16*, 182.
26. Naha, P. C.; Casey, A.; Tenuta, T.; Lynch, I.; Dawson, K. A.; Byrne, H. J.; Davoren, M. *Aquat. Toxicol.* **2009**, *92*, 146.
27. Tauer, K.; Gau, D.; Schulze, S.; Völkel, A.; Dimova, R. *Colloid Polym. Sci.* **2009**, *287*, 299.
28. Liu, C. Y.; Li, L.; Qiu, F.; Yang, Y. *Acta Chim. Sin.* **2010**, *68*, 1325.
29. Yi, C. L.; Yang, Y. Q.; Zhu, Y.; Liu, N.; Liu, X. Y.; Luo, J.; Jiang, M. *Langmuir* **2012**, *28*, 9211.
30. Garcia-Carbonero, R.; Supko, J. G. *Clin. Cancer Res.* **2002**, *8*, 641.
31. Liu, J.; Lee, H.; Allen, C. *Curr. Pharm. Des.* **2006**, *12*, 4685.